Electronic Supporting Information

Microsphere-Supported Gold Nanoparticles for SERS detection of Malachite Green

*David T. Hinds,[a] Samir A. Belhout,[a] Paula E. Colavita,[b] Andrew D. Ward, and Susan J. Quinn[a]**

a. School of Chemistry, University College Dublin, Belfield, Dublin 4, Ireland.

b. School of Chemistry and CRANN, Trinity College Dublin, College Green, Dublin 2, Ireland

c. Central Laser Facility, Research Complex at Harwell, STFC Rutherford Appleton Laboratory,
Harwell Oxford, Didcot, Oxfordshire, OX11 0FA, UK.

*Corresponding Author email: susan.quinn@ucd.ie

Preparation of Gold Nanoparticles

Aqueous 4-Dimethylaminopyridine stabilized AuNPs were prepared by the Gittins phase transfer method[1]. An aqueous solution (30 mM, 30 ml) of $HAuCl_4{\cdot}3H_2O$ in diH_2O, was added to a solution (25 mM, 80 ml) of tetraoctylammonium bromide (TOAB) in toluene. To this, a fresh solution (0.4 M, 25 ml) of $NaBH_4$ was added under stirring. After 30 min the toluene phase was washed with H_2SO_4 (0.1 M), NaOH (0.1 M) and three times with diH_2O before drying over anhydrous Na_2SO_4. An aqueous solution (0.1 M) of 4-dimethylaminopyridine (DMAP) was added to aliquots of TOAB stabilized nanoparticles in a 1:1 ratio by volume. Phase transfer was allowed to proceed, without stirring, until the toluene phase appeared clear and the aqueous phase had developed a deep ruby red color.

Borohydride anion stabilized AuNPs were prepared with minor modification to the synthesis outlined by Martin *et al.*[2] A 1 mL aqueous solution of $NaBH_4$ (50 mM) containing an equimolar amount of NaOH. 9.6 g of water was placed in a 20 mL glass beaker and shaken at 800 rpm at room temperature. To this 100 µL of a solution containing $HAuCl_4$ (50 mM) and HCl (50 mM) was added and the solution allowed to mix for 30 s before the addition of 320 µL of a solution containing $NaBH_4$ (50 mM) and NaOH (50 mM).

Characterization techniques. Scanning electron microscope (SEM) images were collected using a Zeiss Ultra Plus microscope with an In-lens detector at the AML facility of the CRANN institute, Trinity College Dublin. Analysis of diameter of the cluster sizes after hydroquinone treatment was carried out using ImageJ software. Due to their irregular shape, the outline of clusters was traced using the free hand function and the Feret diameter of the cluster was determined. This was performed on both DMAP (n=97) and borohydride (n=107) stabilised systems. ζ-potential measurements were carried out on a Malvern Zetasizer Nano-ZS, equipped with a 4 mW He-Ne laser operating at 632.8 nm, measurements were taken at 173°; NaCl was added of in order to bring the total ionic strength to a value of 0.010 M. The sample was pre-treated at 30 °C under vacuum for 24 h prior to analysis using nitrogen as the adsorbing gas. UV-visible absorbance was measured on a Varian, Cary 50 Eclipse spectrophotometer at room temperature. All UV-Vis measurements were made in a quartz cell, except DMAP-Au samples which were measured in disposable plastic cells.

Schemes and Figures

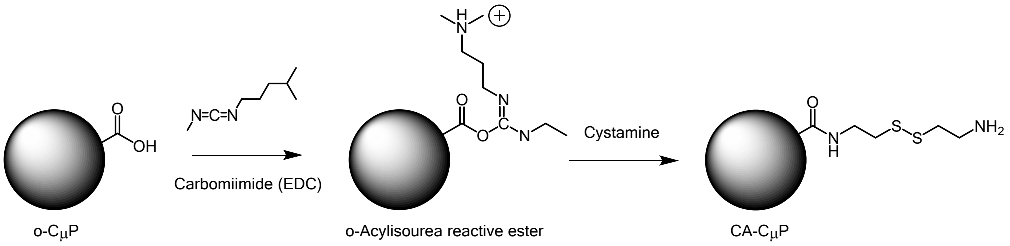

Scheme S1. Reaction scheme for the preparation of cystamine functionalized **CA-CµP**.

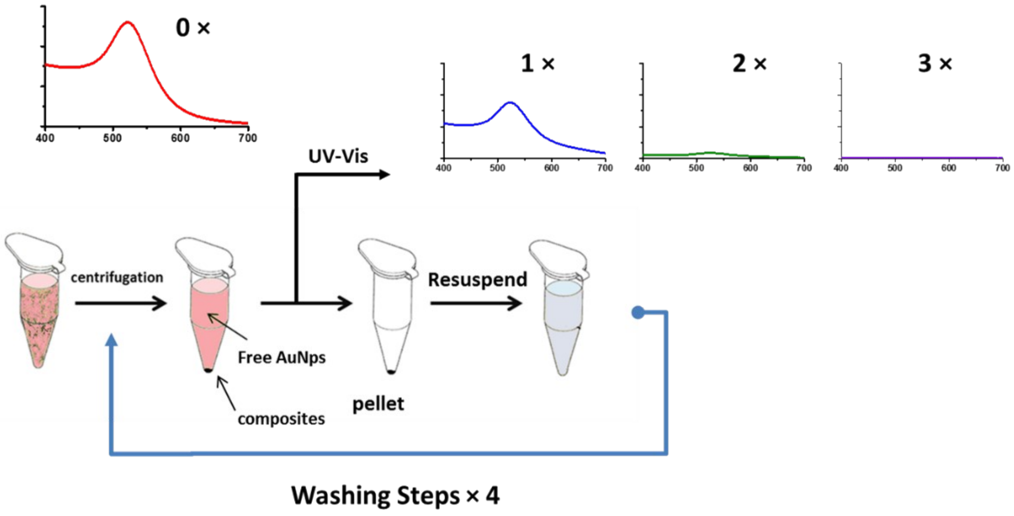

Scheme S2. Schematic of centrifugation washing showing visible absorption spectra of the supernatant of composite solutions following successive washing steps and SEM micrograph of composites following four washing steps.

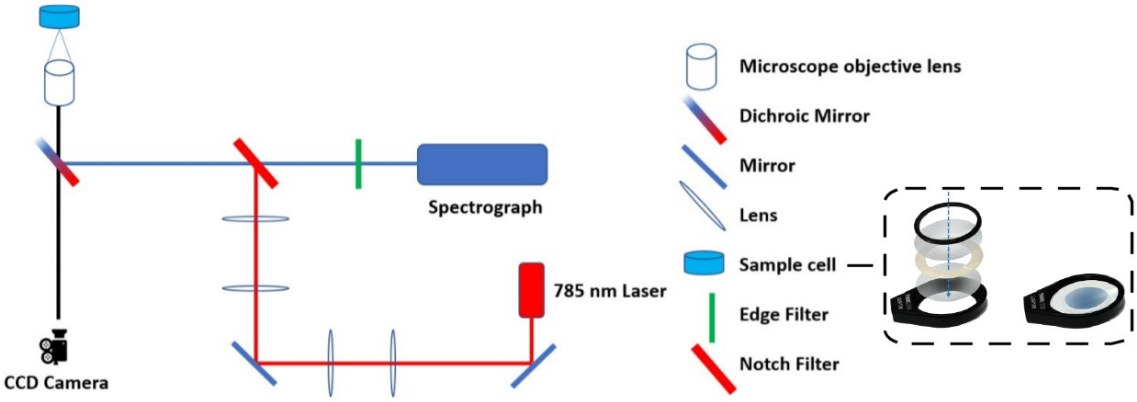

Scheme S3. Schematic representation of set-up for single particle Raman measurements

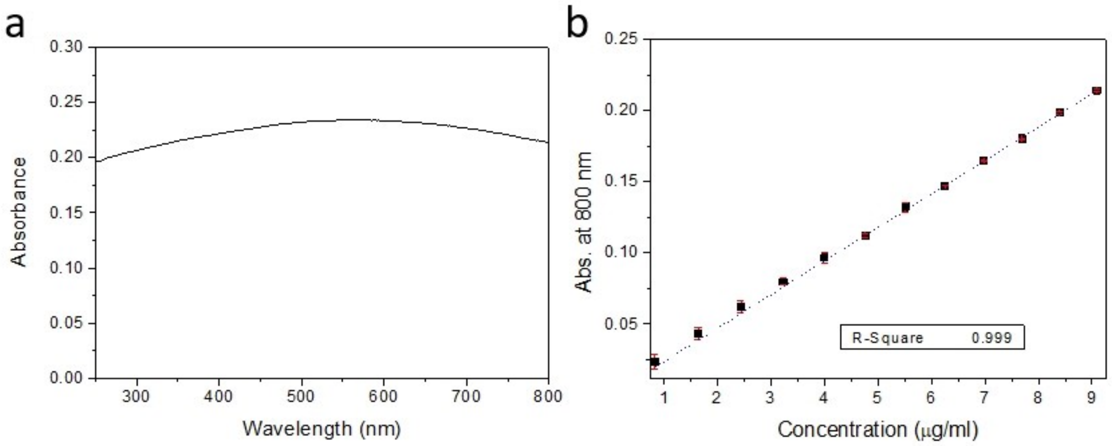

Figure S1: (a) Absorbance spectrum of an aqueous dispersion of CμP; and **(b)** Linear fit of absorption at 800 nm vs. concentration of CμP (error bars show standard deviation from three measurements). Spectra recorded in ddiH_2O at rt.

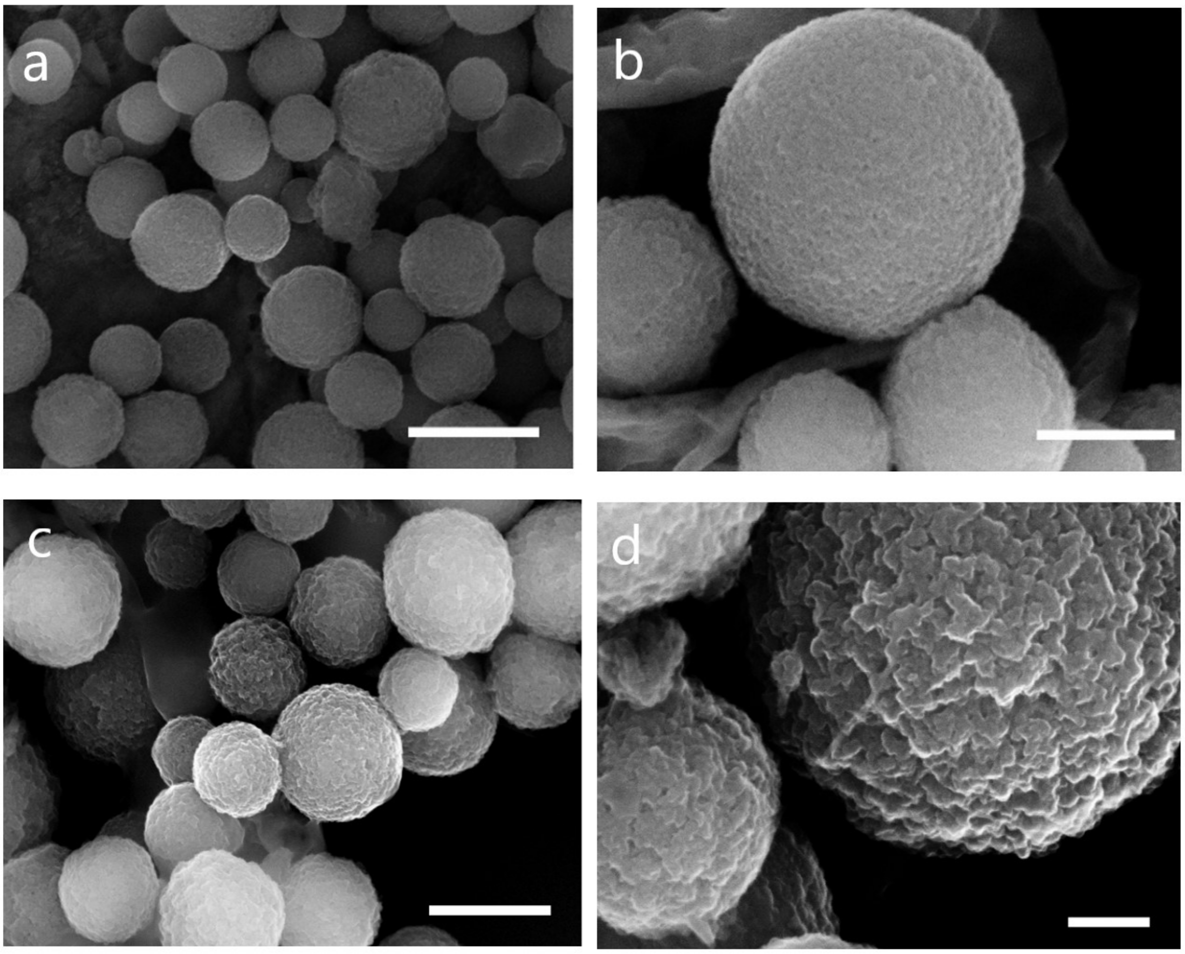

Figure S2: SEM micrographs of **(a-b) o-CμP** formed by reacting in 5 M HNO_3 at 80 °C for 2 h. Scale bars are 1 μm (RHS) and 500 nm (LHS) respectively. **(c-d) CA-CμP**. Scale bars show (c) 1 μm and (d) 200 nm.

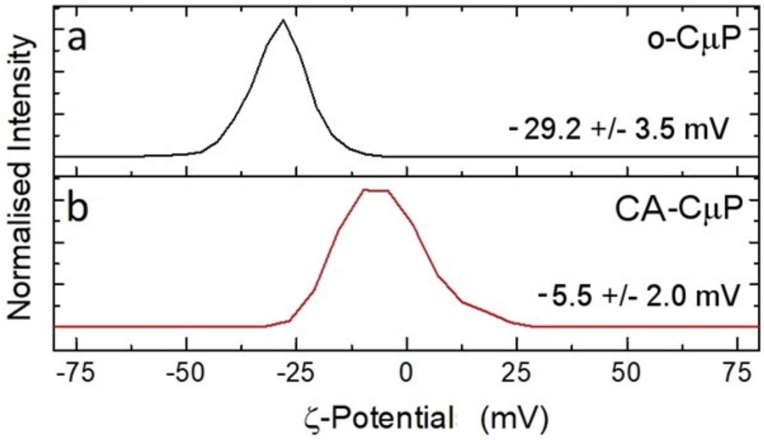

Figure S3: ζ-potential measurements of (a) **o-CμP** and (b) **CA-CμP** recorded in 10 mM NaCl at pH 7.

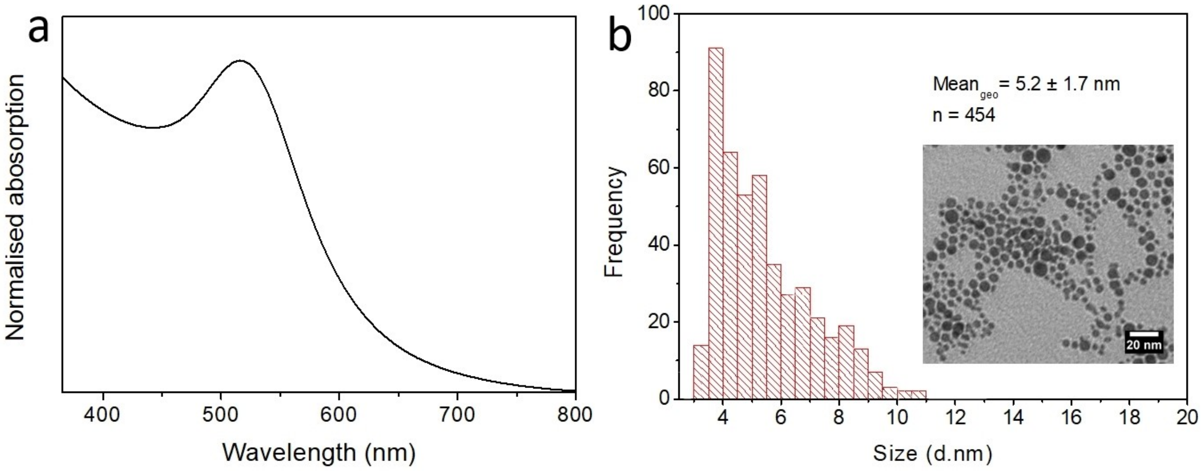

Figure S4: (a) Normalized absorption spectrum of AuNP(DMAP) in ddiH_2O. (b) TEM micrograph size distribution analysis of AuNP(DMAP) nanoparticle. Insert: TEM micrograph of these nanoparticles.

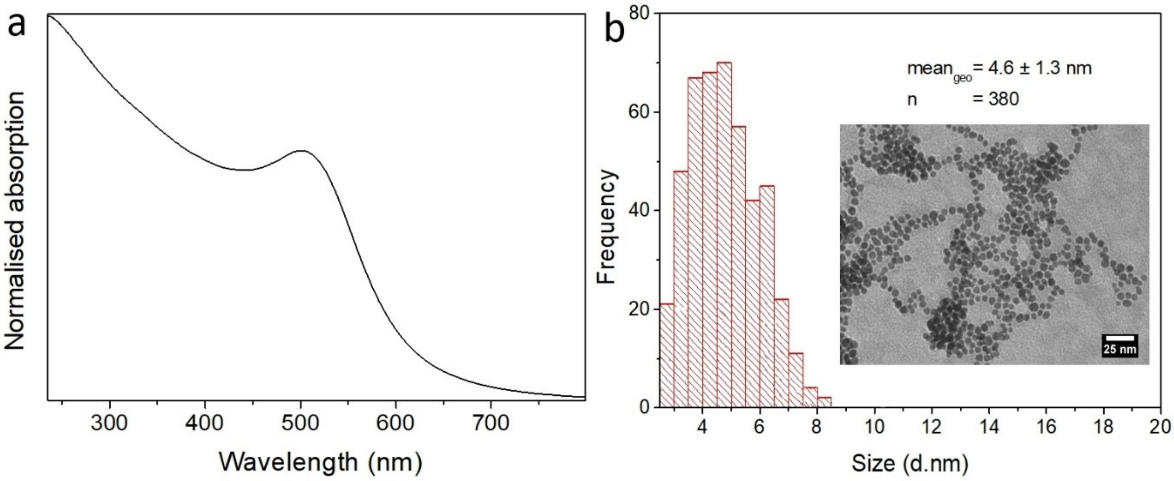

Figure S5. (a) Normalised absorption spectrum of AuNP(BH) in ddiH_2O. (b) TEM micrograph size distribution analysis of AuNP(BH). Insert is a TEM micrograph of these nanoparticles.

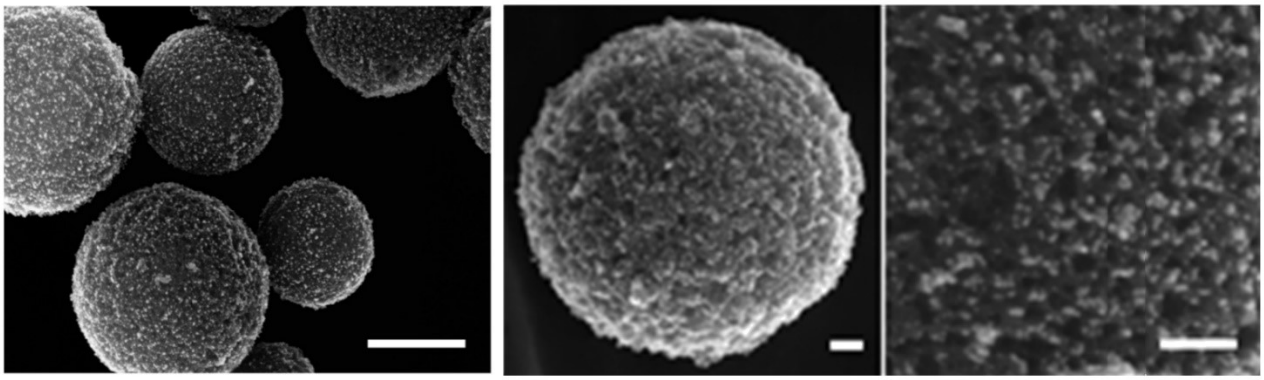

Figure S6. Additional representative SEM micrographs of **CµP-AuNP(DMAP)** composites. Scale bars shows (a) 500 nm (b-c) 100 nm.

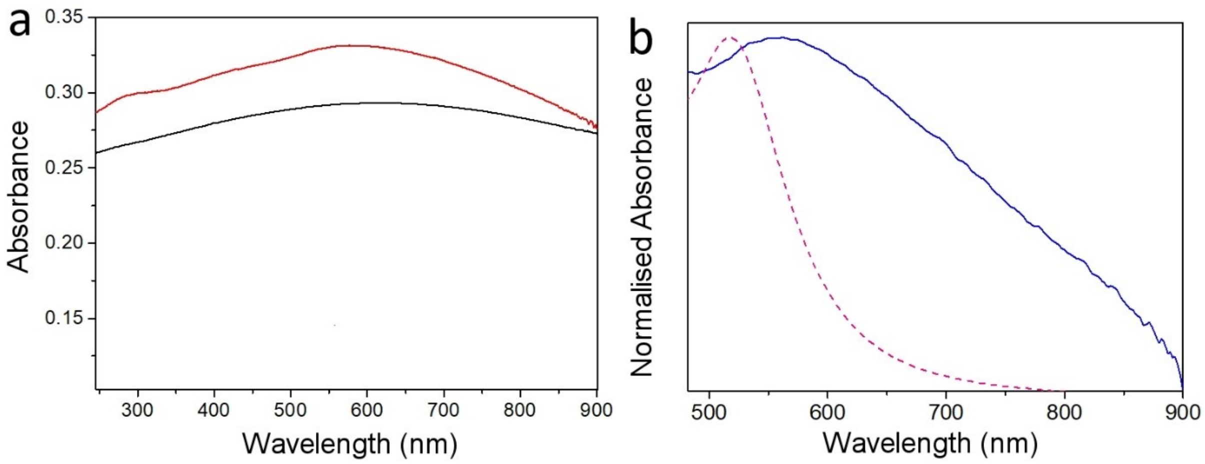

Figure S7 UV-Vis spectra of **(a) o-CµP** (black trace) and **CµP-AuNP(DMAP)** (red trace); and **(b)** AuNP(DMAP) (red trace) and difference spectrum (blue trace). Spectra recorded in ddiH_2O in a quartz cuvette.

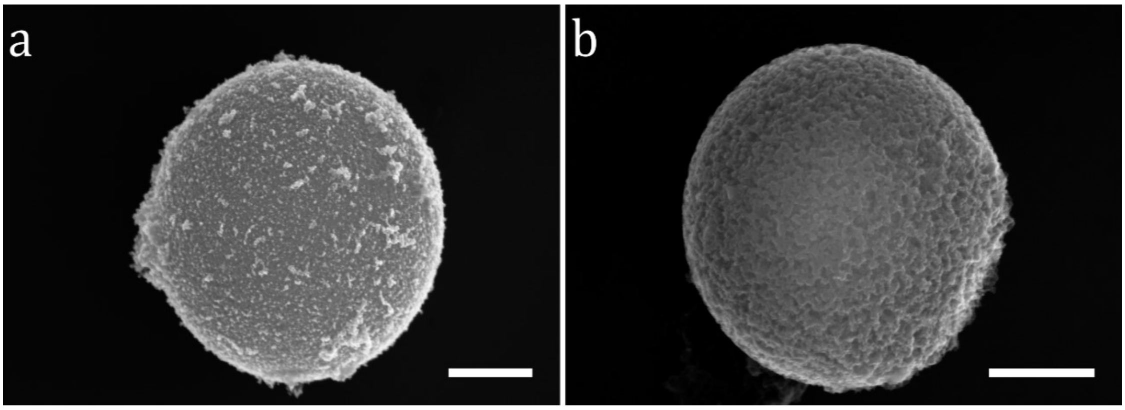

Figure S8. CµP-AuNP(DMAP) (a) before; and **(b)** after; gold digestion by sonication in 5 % aqua regia solution**.** Scale bars show 500 nm.

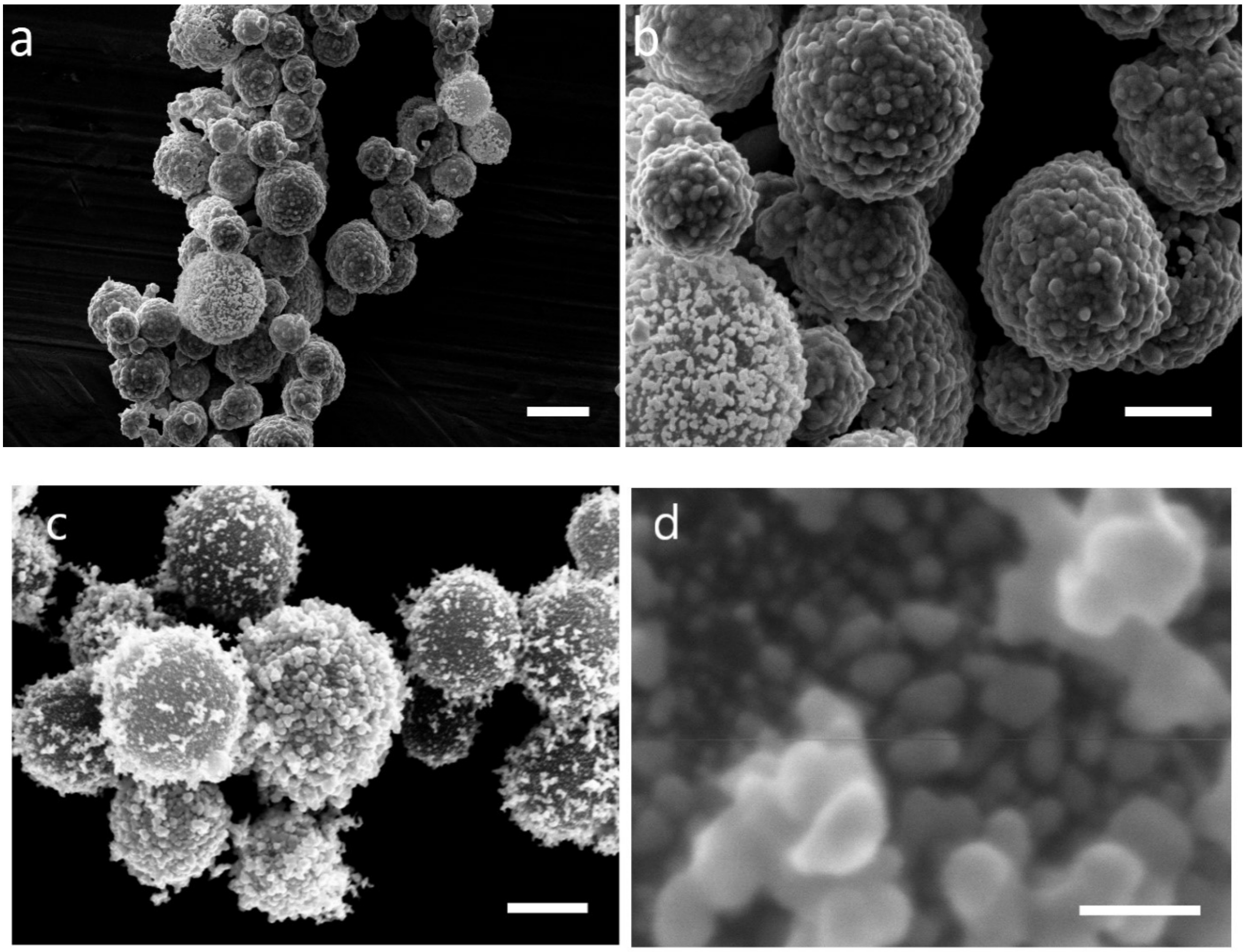

Figure S9. SEM micrographs of Hydroquinone/HAuCl$_4$ treated **CμP-AuNP(DMAP)** composite particles **CμP-AuNP-1**. Scale bars show; (a) 1 μm; (b, c) 500 nm and (d) 50 nm.

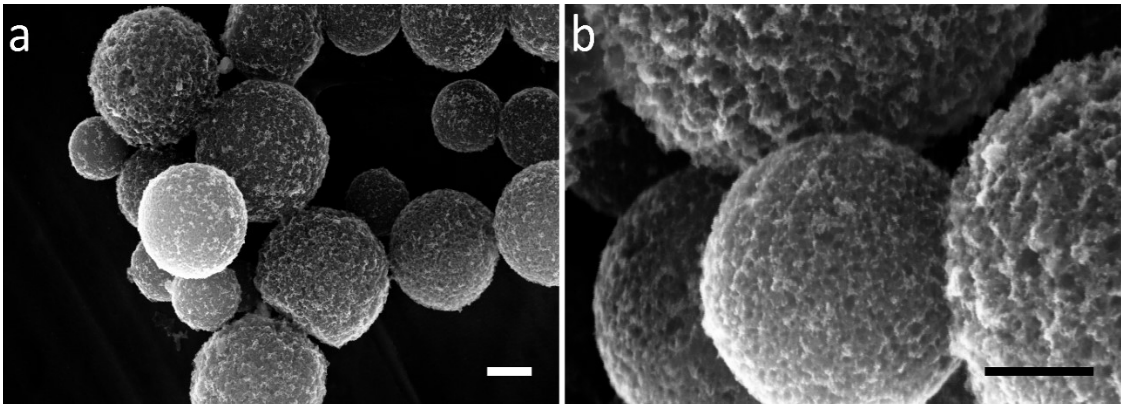

Figure S10. Additional representative SEM micrographs of **CμP-AuNP(BH)** composites. (Scale bars show; **(a)** 500 nm; and **(b)** 200 nm).

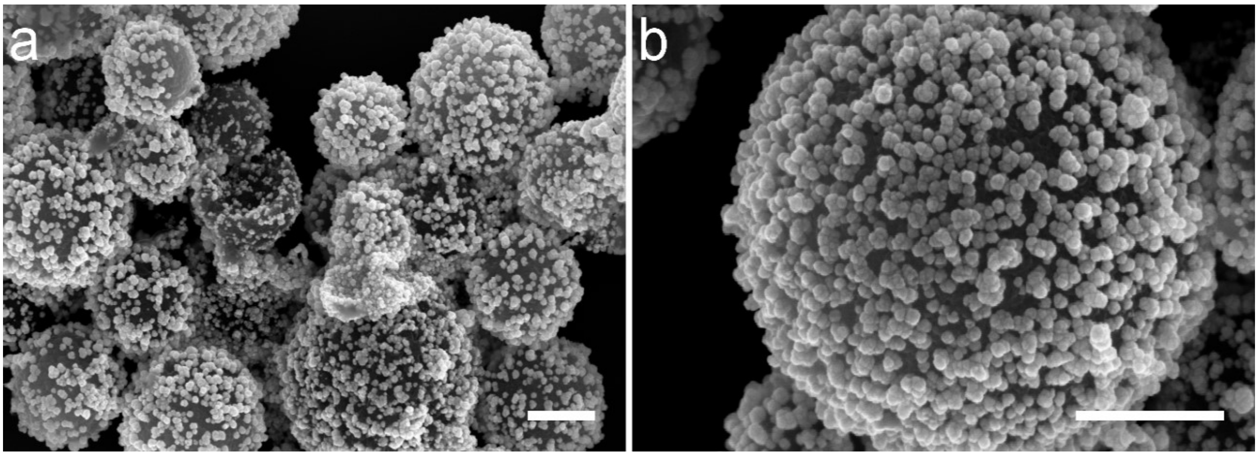

Figure S11. SEM micrographs of **CµP-AuNP-2** composite particles. Scale bars show **(a)** 500 nm; and **(b)** 500 nm.

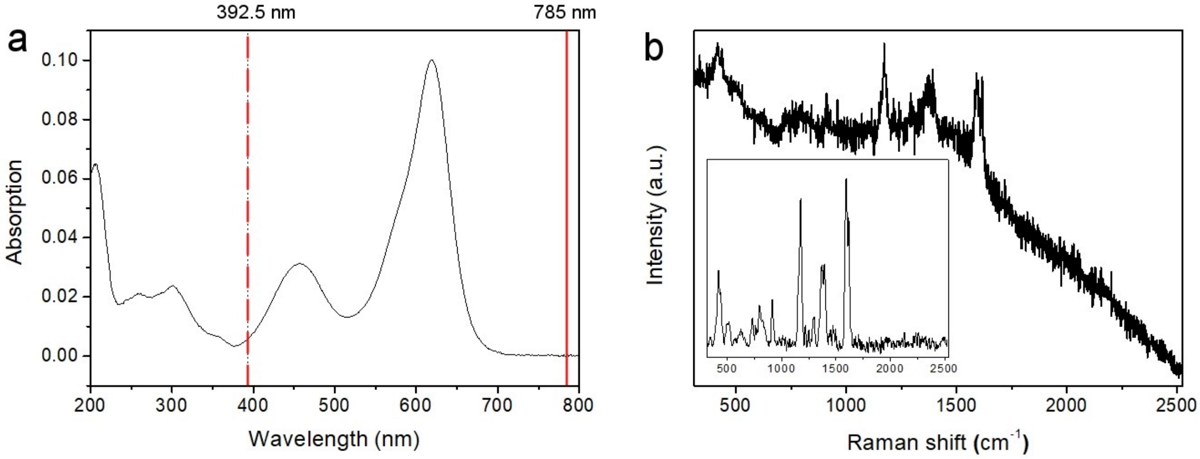

Figure S12. (a) UV-Vis absorption spectrum of malachite green isothiocyanate. Solid line shows laser excitation wavelength, dashed line shows the two photon wavelength of this laser. (Recorded in diH_2O). **(b)** Raman spectrum of solid film of malachite green drop cast from 1 mM MG solution in ethanol with 785 nm excitation. Insert shows spectrum following smoothing and baseline correction.

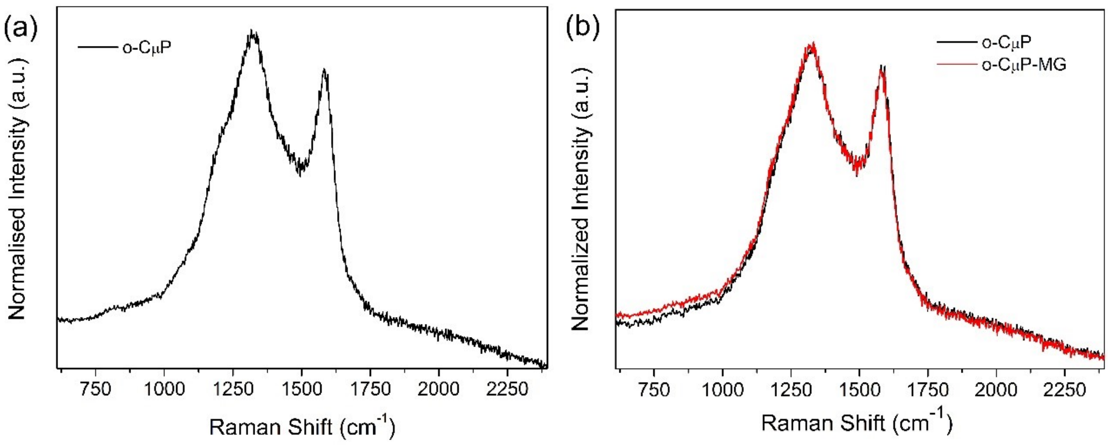

Figure S13. Normalized Raman spectra for (a) an optically trapped **o-CμP** particle recorded in H_2O with 785 nm excitation. (b) Comparison recorded for **o-CμP** incubated in the presence of 10 μM MG.

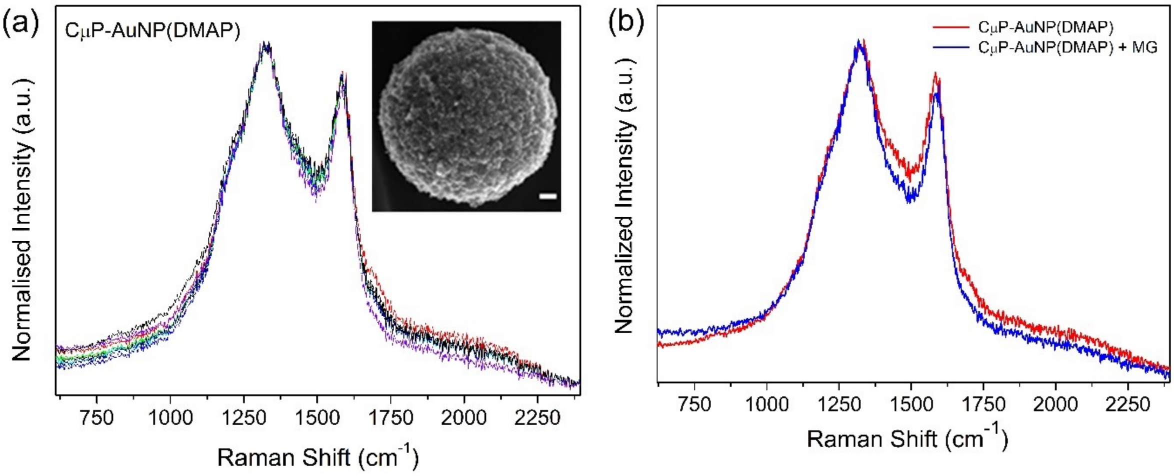

Figure S14. Normalized Raman spectra for (a) **CμP-AuNP(DMAP)** composite particles, inset showing the SEM image with a scale bar of 100 nm, and (b) **CμP-AuNP(DAMP)** incubated with 10 μM MG recorded in H_2O with 785 nm excitation.

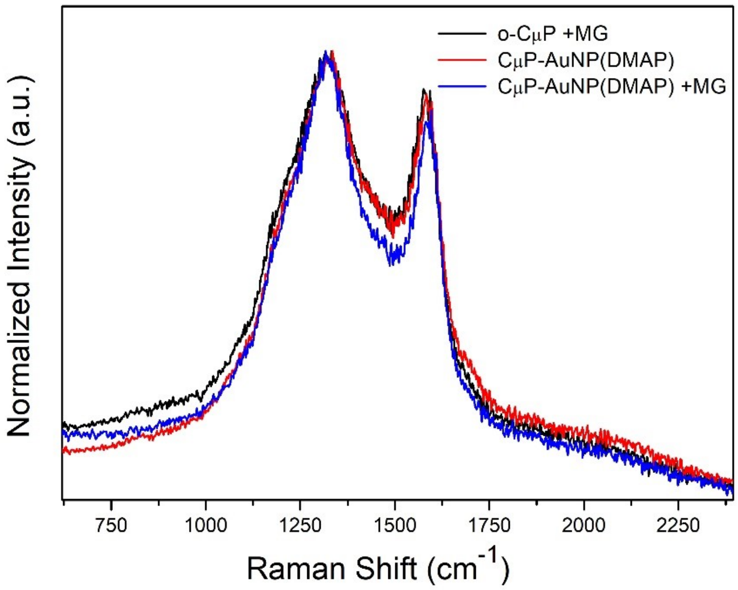

Figure S15. Normalized Raman spectra for an optically trapped (a) **o-CμP** incubated with 10 mM MG. (b) **CμP-AuNP(DMAP)** composite particle and (c) **CμP-AuNP(DAMP)** incubated with 10 mM MG recorded in H_2O with 785 nm excitation.

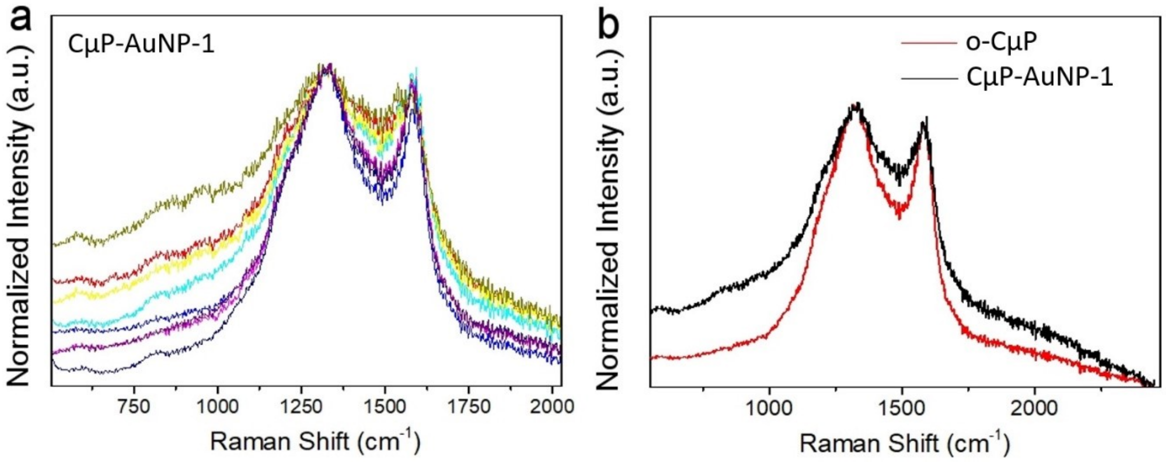

Figure S16. (a) Normalized Raman spectra for a selection of **CμP-AuNP-1** particles, showing the variable dampening in carbon D and G bands. Each trace shows an individual particle. (b) Averaged normalized Raman spectra of o-CμP particles (red trace) and **CμP-AuNP-1** particles (black trace) Spectra recorded in H_2O with 785 nm excitation.

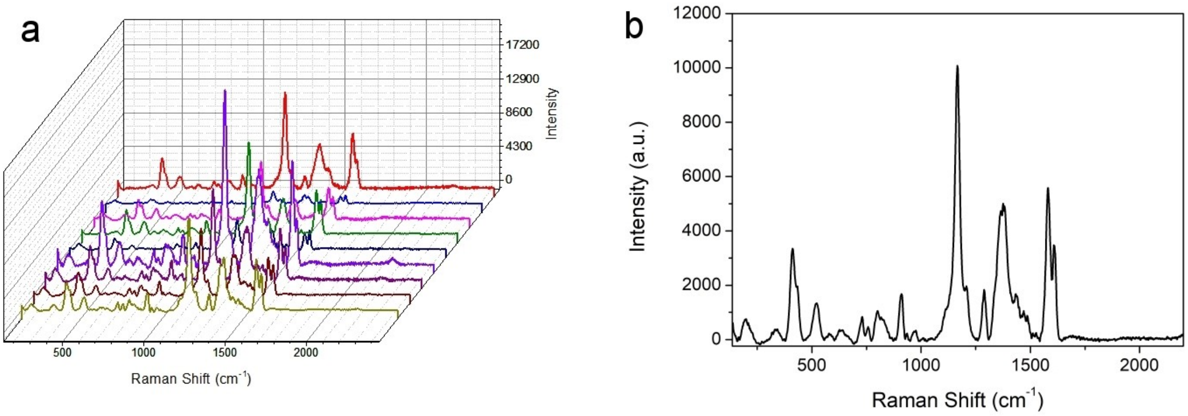

Figure S17. (a) Analyte Raman spectrum from **CμP-AuNP-1** composite particles incubated with 10 μM MG. Each trace shows an individual particle. (b) Average SERS spectrum from all measured particles.

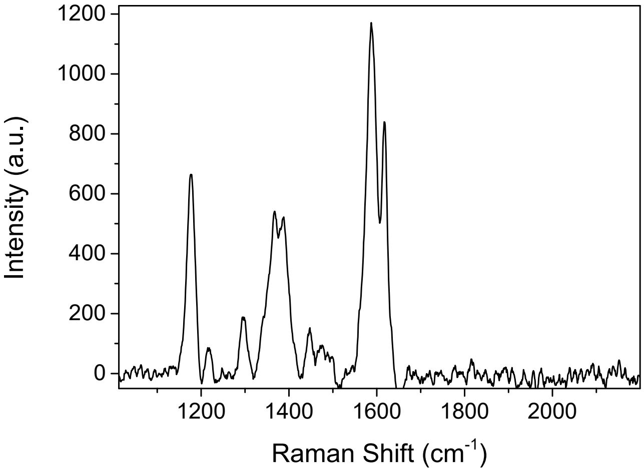

Figure S18. Bulk solid Raman spectrum from 10 μM MG-incubated **CμP-AuNP-1** particles. Spectra recorded with 514 nm excitation from a sample drop cast on CaF_2.

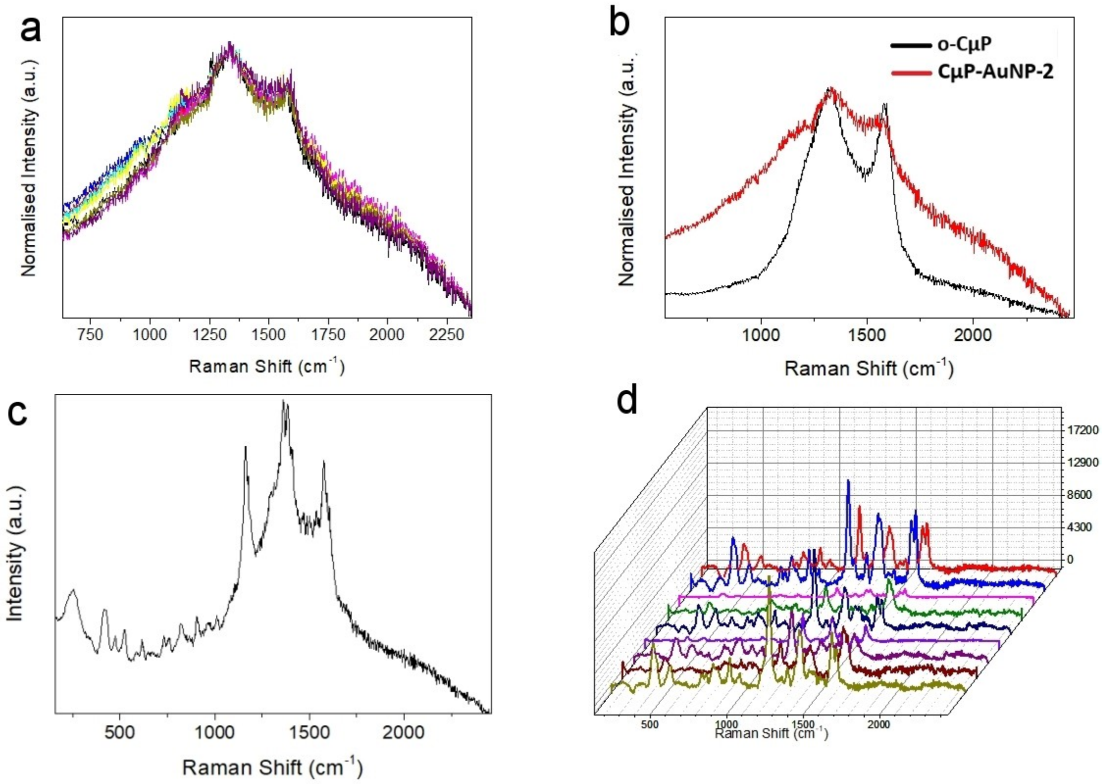

Figure S19 (a) Normalized Raman spectra for eight **CμP-AuNP-2** particles. (b) Averaged normalized Raman spectra of **CμP-AuNP-2** particles (black trace) **o-CμP** particles (red trace). (c) Raman spectrum from trapped **CμP-AuNP-2** composite particle incubated with 10 μM **MG**. (d) Raman spectrum **CμP-AuNP-2** composite particles incubated with 10 μM MG. Each trace shows an individual particle. Spectra recorded in H_2O with 785 nm excitation.

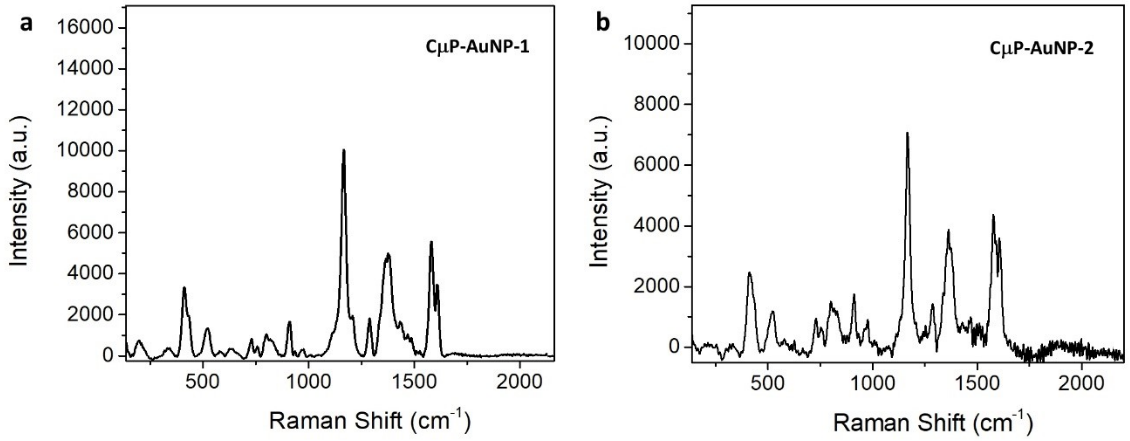

Figure S20. Averaged Raman spectra of (a) **CμP-AuNP-1** and (b) **CμP-AuNP-2** recorded for particles incubated with 10 μM MG. Spectra recorded in H_2O with 785 nm excitation.

Table S1. Summary of the properties of AuNP systems

Family	**AuNP-DMAP**	**AuNP-BH**
Size by TEM	5.2 ± 1.7 nm (n =454)	4.6 ± 1.3 nm (n =380)
ζ-potential	+28.3± 1.2 mV (n =3)	−20± 2.0 mV (n =3)
λ_{max}	512 nm	508 nm

Table S2 List of Raman peaks for CμP-AuNP-1, and CμP-AuNP-1incubated with malachite green isothiocyanate

CμP-AuNP-1	**CμP-AuNP-2**	**Solid MG**	**Literature values[3],***	**Asignment[3]**
Raman shift (cm$_{-1}$)				
			226 m	C-ϕ_3 breathing ϕ-C-ϕ bend
415		416	412 sh	O.o.p benzene
	422	436	438 s	ring deformation,
	474		462 w	e_{2u}
525	522		530 m	I.p. benzene
	592		578 w	ring deformation,
	620		626 w	e_{2g}
			662 w	
728	730	729	734 w	I.p. benzene ring bend, stretch
	761	758	761 m	NR, bend, torsion
800	824		806 s	O.o.p. C-H (benzene e_{1g})
910	910	911	918 s	I.p. benzene b_{1u}
			942 w	$N(CH_3)_2$, stretch, bend
			988w	I.p. benzene e_{1u}
			1000 w	I.p. benzene e_{1u}
1169	1163	1172	1176 s	I.p. C-H bend
1210			1221 s	N-C stretch, NR_2 bend
1285		1297	1297 s	I.p. C-C and C-C-H
			1340 m	Combination
	1364	1367	1368 m	N-ϕ stretch
	1385		1402 s	I.p. C-C, C-H
			1449 s	NR_2 bend and rock
			1492 m	NR_2 bend and rock
1578	1575	1590	1596 s	I.p. ring stretch, bend
1616	1607	1618	1619 s	N-ϕ and C-C strech

O.o.P. = out-of-plane; I.p. = in-plane.
* solution measurements from reference [9] (5 × 10^{-4} M, 514 nm laser excitation)

References

1. D. I. Gittins, F. Caruso, *Angew. Chemie Int. Ed.* 2001, **40**, 3001–3004.
2. M. N. Martin, J. I. Basham, P. Chando, S. K. Eah, Langmuir 2010, **26**, 7410–741.
3. H. B. Lueck, D. C. Daniel, J. L. McHale, *J. Raman Spectroscs.* 1993, **24**, 363–370.